Heart rate monitoring via remote photoplethysmography with motion artifacts reduction

Giovanni Cennini[1]*, Jeremie Arguel[2], Kaan Akşit,[1,3], and Arno van Leest[1]

[1]*Philips Research, HTC 34, 5656AE Eindhoven, The Netherlands*
[2]*ENSEEIHT, University of Toulouse, 2 rue Camichel, 31071 Toulouse Cedex 7, France*
[3]*RWTHAachen, Templergraben 55, 52062 Aachen, Germany*
**giovanni.cennini@philips.com*

Abstract: In this paper, we present a novel photoplethysmographic device that operates remotely, i.e. not in contact with the skin. The device allows for real time measurements of heart rate with motion artifact reduction from a distance of a few centimeters up to several meters. High mobility of users is achieved in assessment of vital body signs, such as heart rate.

OCIS codes: (230.0230) Optical devices; (280.4788) Optical sensing and sensors; (170.3890) Medical optics instrumentation.

References and links

1. A. B. Hertzman, "Photoelectric plethysmograph of the fingers and toes in man," Proc. Soc. Exp. Biol. Med. **37**, 529 (1937).
2. T. Aoyagi, "Pulse oximetry: its invention, theory, and future," J. Anesth. **17**(4), 259–266 (2003).
3. J. W. Severinghaus, and P. B. Astrup, "History of blood gas analysis. VI. Oximetry," J. Clin. Monit. **2**(4), 270–288 (1986).
4. J. W. Severinghaus, and Y. Honda, "History of blood gas analysis. VII. Pulse oximetry," J. Clin. Monit. **3**(2), 135–138 (1987).
5. W. G. Webster, J. G. Webster, and R. Ed Webster, *Design of Pulse Oximeters*, (Taylor & Francis Group, 1997).
6. T. Wu, "PPGI: New Development in Noninvasive and Contactless Diagnosis of Dermal Perfusion Using Near InfraRed Light," J. GCPD e. **7**(1), 17 (2003).
7. N. Blanik, M. Hülsbusch, M. Herzog, and C. R. Blazek, "Assessment of Human Hemodynamics under Hyper- and Microgravity: Results of two Aachen University Parabolic Flight Experiments," Acta Polytechnica **47**(4), 29 (2007).
8. J. Zheng, S. Hu, V. Azorin-Peris, A. Echiadis, V. Chouliaras, and R. Summers, "Remote simultaneous dual wavelength imaging photoplethysmography: a further step towards 3-D mapping of skin blood microcirculation," Multimodal Biomedical Imaging III, Proc. SPIE **6850**, 68500S (2008).
9. K. Humphries, T. Ward, and C. Markham, "A CMOS Camera-Based Pulse Oximetry Imaging System", in Proceedings of the 2005 IEEE Engineering in Medicine and Biology 27th Annual Conference Shanghai, China, 1–4 September, 2005
10. K. Humphreys, T. Ward, and C. Markham, "Noncontact simultaneous dual wavelength photoplethysmography: a further step toward noncontact pulse oximetry," Rev. Sci. Instrum. **78**(4), 044304 (2007).
11. F. P. Wieringa, F. Mastik, and A. F. W. van der Steen, "Contactless multiple wavelength photoplethysmographic imaging: a first step toward "SpO2 camera" technology," Ann. Biomed. Eng. **33**(8), 1034–1041 (2005).
12. W. Verkruysse, L. O. Svaasand, and J. S. Nelson, "Remote plethysmographic imaging using ambient light," Opt. Express **16**(26), 21434–21445 (2008P).
13. P. Shi, S. Hu, A. Echiadis, V. Azorin-Peris, J. Zheng, and Y. Zhu, "Development of a remote photoplenthysmographic technique for human biometrics," Design and Quality for Biomedical Technologies II, edited by Ramesh Raghavachari, Rongguang Liang, Proc. SPIE **7170**, 717006 2009.
14. L. H. Norton, B. Squires, N. P. Craig, G. McLeay, P. McGrath, and K. I. Norton, "Accuracy of pulse oximetry during exercise stress testing," Int. J. Sports Med. **13**(7), 523–527 (1992).
15. H. Benoit, F. Costes, L. Feasson, J. R. Lacour, F. Roche, C. Denis, A. Geyssant, and J. C. Barthélémy, "Accuracy of pulse oximetry during intense exercise under severe hypoxic conditions," Eur. J. Appl. Physiol. Occup. Physiol. **76**(3), 260–263 (1997).
16. M. J. Hayes, P. R. Smith, D. M. Barnett, M. D. L. Morgan, S. Singh, and D. D. Vara, "Quantitative investigation of artifact in photoplethysmography and pulse oximetry for respiratory exercise testing," in Proceedings of the Seventh International Symposium CNVD Computer-aided Noninvasive Vascular Diagnostics, V. Blažek and U. Schultz-Ehrenburg, ed. (VDIVerlag, Düsseldorf, Germany), 263, 117, 1998.

#121098 - $15.00 USD Received 7 Dec 2009; revised 4 Feb 2010; accepted 17 Feb 2010; published 24 Feb 2010

17. C. M. Lee, and Y. T. Zhang, "Reduction of motion artifacts from photoplethysmographic recordings using a wavelet denoising approach", Biomedical Engineering, IEEE-EMBS Asian-Pacific Conference,194, 2003.
18. K. W. Chan, and Y. T. Zhang, ""Adaptive Reduction of Motion Artifacts from Photoplethysmography recording using a Variable Step-size LMS Filter", Sensors 2002," Proc. IEEE **2**, 1343 (2002).
19. H. Han, M. J. Kim, and J. Kim, "Development of real-time motion artifact reduction algorithm for a wearable photoplethysmography", in *Proceedings of the 29th Annual International Conference of the IEEE EMBS*, 1538, 2007.
20. H. H. Asada, P. Shaltis, A. Reisner, S. Rhee, and R. C. Hutchinson, "Mobile monitoring with wearable photoplethysmographic biosensors," IEEE Eng. Med. Biol. Mag. **22**(3), 28–40 (2003).
21. http://omlc.ogi.edu/spectra/hemoglobin/index.html
22. R. Winston, J. C. Miñano, and P. Benítez, *Nonimaging Optics*, (Elsevier Academic Press, 2005).
23. D. Thompson, A. Wareing, D. Day, and S. Warren, "Pulse Oximeter Improvement with an ADC-DAC Feedback Loop and a Radial Reflectance Sensor"', in *28th Annual International Conference of the IEEE Engineering in Medicine and Biology Society*, 815, 2006.
24. USB Framework for PIC18, PIC24 $\&$ PIC32, Microchip, *http://www.microchip.com*
25. J. R. Barry, E. A. Lee, and D. G. Messerschmitt, *Digital Communication: Third Edition*, (Kluwer Academic Publishers, 2004).

1. Introduction

Monitoring of vital body signs such as heart rate and blood oxygenation via photoplethysmography (PPG) originates from early investigations of Hertzman on blood circulation in limb extremities [1]. Today, pulse oximeters are widely accepted monitoring devices based on contact photoplethysmography, i.e. sensors and light sources that are in contact with the tissues under investigation [2–5]. Although successful, current photoplethysmographs are not preferred in situations with poor hygiene control, sensitive skin, damaged skin, or in case of freedom of movement of people.

Possible attempts to overcome the contact with the skin have been explored by photoplethysmography imaging, a diagnostic technique that assesses blood perfusion in skin layers [6–8]. Humphries *et al*. [9,10] and Wierenga have shown that multispectral imaging can be a first step towards 2D maps of analyte concentration in skin [11]. Recently, it has been shown that analysis of video from an RGB camera using ambient illumination leads to results similar to photoplethysmography imaging [12].

On the other hand, using simple sensors such as photodiodes allows for fast, cheap, and high dynamic acquisition of photoplethysmographic signal from the tissues of the skin. Shi *et al*. have indeed demonstrated a non-contact photoplethysmograph using infrared LED illumination and a simple photodiode [13]. However, in that pioneering work motion artifacts were not dealt with and the system operated in still conditions requiring no motion of the subject. This leads to a limited range of applications for the system. We anticipate that extensive acceptance of remote photoplethysmography will happen when the technique reaches the same maturity as contact photoplethysmography.

In this letter, we demonstrate a photoplethysmograph that can measure heart rate from a distance of a few centimeters up to one meter. Real-time motion artifact compensation is demonstrated as well. The device reported on here is based on photodiodes. This represents a low cost solution with high sensitivity and extremely fast response with respect to high-speed state-of-art cameras.

2. Remote photoplethysmography and motion artifacts compensation

Motion has been clinically demonstrated to cause errors in pulse oximeters response [14–16]. In contact photoplethysmography, displacement of light sources with respect to the detector, non-optimal optical coupling and variation of motion-induced hemodynamics represent the main causes of artifacts. Several techniques have been investigated to cope with those artifacts, such as analysis of the pulsation components in frequency and time domain [17,18] or the use of the wavelet de-noising method [19]. Other approaches are based on processing context information by additional on-body sensors and light sources [20].

#121098 - $15.00 USD Received 7 Dec 2009; revised 4 Feb 2010; accepted 17 Feb 2010; published 24 Feb 2010

In case of remote photoplethysmography, because sensors and light sources are detached from the skin the variations of the light intensity registered by the sensors as result of motion are far more severe than the corresponding ones in ordinary PPG devices. Indeed, the amplitude of motion that we consider in our setup is such that the motion itself becomes the dominant signal; see Fig. 1 for a typical example of PPG signal acquired with our device. We point out that the aforementioned motion artifacts compensation techniques are *per se* not effective when applied alone.

Figure 1 shows a typical PPG signal acquired with our remote photoplethysmograph device without motion artifacts compensation. The measurements were taken when one of the authors aimed his palm at the sensor from a distance of 30 cm in ambient light conditions. The first and the last part of the signal display a clear blood volume pulses characteristics when the subject did not move his palm. The mid part of the signal displays severe artifacts and corresponds to rotation of the hand of about 3 degree with an oscillation of the palm of about 3 Hz.

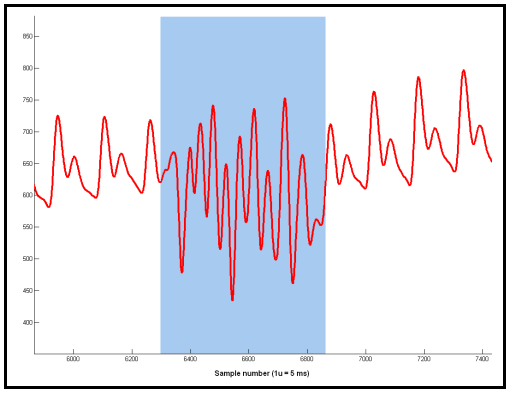

Fig. 1. PPG signal with motion artifacts. The signal was taken at a distance of 30 cm. The first and last parts of

the signal show clear blood volume pulse characteristics. The central part is corrupted by motion. The motion has a frequency of about 3 Hz and corresponded to displacement of the hand of approximetely 3°.

In order to mitigate and eventually eliminate these artifacts, we implemented a hybrid approach based on the combination of multi spectral illumination of the region of interest and the use of an adaptive filter. In addition to the actual PPG signal that contains motion artifacts (S_{PPG+M}), we recorded a signal proportional to the motion of the skin (S_M). This double signal detection is obtained using a dual-wavelength illumination of the region of the interest. In our experiments, the S_{PPG+M} signal is obtained with blue light, as the hemoglobin protein strongly absorbs in the blue region of the visible spectrum. The signal containing the motion information S_M is obtained by illuminating the region of interest using infrared light, as absorption by hemoglobin in that spectral range is lower. The ratio of the light absorption by hemoglobin in the two spectral region of interest is estimated via the Eq. (1):

$$\frac{\alpha_{HbO/Hb}(\lambda_1)}{\alpha_{HbO/Hb}(\lambda_2)} \approx 500 \qquad (1)$$

where $\alpha_{HbO/Hb}(\lambda_i)$ are the molar extinction coefficients of the oxygenated and deoxygenated hemoglobin at λ_i (cm^{-1}/Mol), see for example [21]. In our case, λ_1 and λ_2 are around 450 nm and 970 nm, respectively. With this choice of wavelengths, we expect that the motion signal S_M contains variations in light intensity that are caused primarily by the movements of the

#121098 - $15.00 USD Received 7 Dec 2009; revised 4 Feb 2010; accepted 17 Feb 2010; published 24 Feb 2010

skin and not by blood volume pulses. S_M is adaptively subtracted from S_{PPG+M} to allow for heart rate calculation. The algorithm used for the subtraction is an adaptive echo cancelation.

3. Experimental prototype

The device we built can monitor the heart rate of a person with motion artifacts compensation in real time. Three main parts can be identified. First, a light collecting stage has been designed in order to efficiently collect and spatially integrate light from an assigned region of interest of the skin. Subsequently, a low-noise hardware stage has been assembled in order to amplify the PPG signal and to enable real time communication to a PC. In a third stage, we process the signals to extract heart beat. In the following paragraphs, the three parts are described.

3.1 Light collecting stage

The part dedicated to the collection of light is composed of a Compound Parabolic Concentrator (CPC), a set of two photodiodes, and associated wavelength filters mounted on top of the detectors. The CPC is a well known nonimaging optics element often used in solar concentrators and light collimators [22]. The CPC integrates light from a region of interest onto the sensitive area of the photodiodes. In Fig. 2, the light collector stage is presented. The optical filters have cut-off wavelengths at 480 nm and 700 nm. The CPC element has been designed to have an acceptance angle of 15°. The two photodiodes are placed at the exit area of the CPC and their centers are displaced by 5 mm with respect to each other. The exit area of the CPC is about 12 mm. The angular extent of the light ray distribution at the exit area is about ± 90°. By doing so, the light rays emitted by two distinct points sources at a distance in space will be collected and spread onto the two sensitive areas of the photodiodes in a correlated fashion. Given the CPC geometry, this overlap is a function of the angular distribution of the intensity radiated by the skin (that we assumed to be a Lambertian distribution), and of the distance between the CPC and the skin.

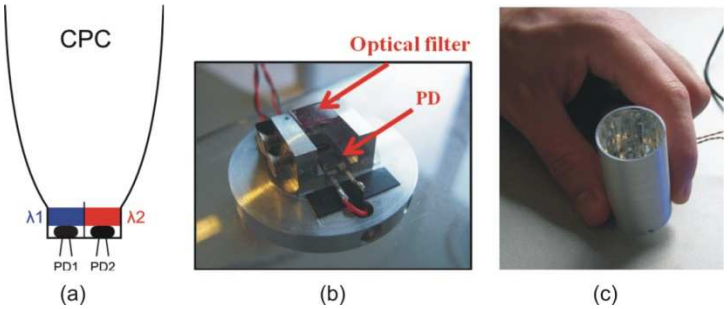

Fig. 2. Light collector. (a) Scheme of the collector stage: sensors (PIN photodiodes), wavelength filters λ_1 and λ_2 and CPC on top of the sensors. (b) Photodiode support. (c) Collector stage as implemented in the experiments.

The sensors are PIN photodiodes (S2506-02, from Hamamatsu, with peak sensitivity at 900 nm). Besides the collecting optics, we have designed a light sources system comprising of two types of LEDs: blue LEDs with a peak emission at 450 nm (Rebel Luxeon from LumiLEDs Philips) and low power infrared LEDs with peak wavelength 970 nm (Roithner Laser). The operating current of the two sets of LEDs has been set in such a way that the current registered by two photodiodes was the same when a reference surface was used.

3.2 Input stage for PPG extraction

For each photodetector, a stage composed of a transimpedance amplifier, a series of analog filters, a DC subtraction operation, and a variable gain amplifier has been implemented. This stage has the task of amplifying the heart-cycled (AC) component of the PPG signal. See Fig.

#121098 - $15.00 USD Received 7 Dec 2009; revised 4 Feb 2010; accepted 17 Feb 2010; published 24 Feb 2010

3 for a schematic view of the hardware. The low-pass filters with cut-off frequency of 5 Hz reduce spurious noise from ambient illumination and increase the signal to noise ratio.

After this filtering, the DC component of the PPG signal is removed using a subtractor and an ADC-DAC (Analog-to-Digital Converter - Digital-to-Analog Converter) feedback loop [23]. The PPG signal and the output of a Digital-to-Analog converter (DAC) are sent to a subtractor. Because the DAC output is equal to the DC component of the PPG, the resulting signal is the AC component of the PPG.

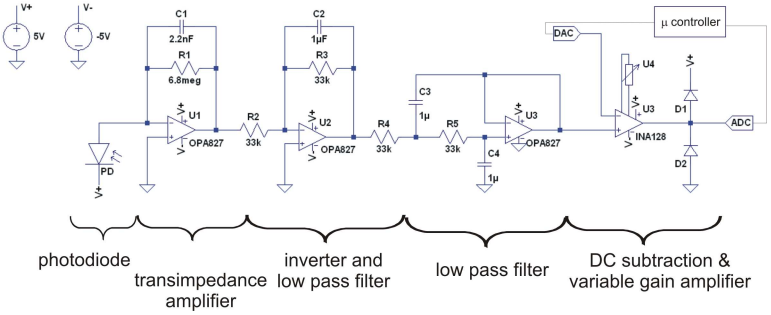

Fig. 3. Electronics scheme of the device for PPG detection.

Analyzing the output of the subtractor (after amplification for better accuracy), the DAC value is adjusted to subtract the correct DC value. The subtractor and the variable gain amplifier are carried out in a single IC. The use of only one component reduces the relative errors in input resistor values (laser trimmed) and overall number of interconnections between several ICs. Thus, it decreases the noise of the circuitry. To turn this amplifier into a variable-gain amplifier, we added a digital potentiometer as a gain resistor (AD5204). The ADC-DAC feedback loop and the digital potentiometer are monitored by a microcontroller (MSP430F2274 from Texas Instruments). A second microcontroller (PIC18F2553 from Microchip), including a 12-bit ADC and an USB module, is used to sample the PPG signal and send it to a PC via USB communication.

Excepting the USB library, the embedded software has been entirely developed in our labs. The sampling is managed by timer interrupts. The USB module communications are performed using the free USB library given by Microchip [24]. The communication between the PC and the microcontroller is directly managed using the software Matlab (MathWorks^{TM}). The Matlab application processes the data sample after sample (filtering and motion compensation), displays the results, and finally requests new data.

3.3 Signal processing

We assumed that the light intensity variations caused by motion of the skin and by the blood volume pulses are additive. This led us to use an adaptive echo cancelation method [25] to reduce the influence of motion. Let us consider S_{PPG} to be the "true" PPG signal, and A the artifacts added to the true PPG signal. If S_{PPG+M} is the corrupted PPG signal (PPG and motion acquired at λ_1), then $S_{PPG+M} = S_{PPG} + A$. We note that S_M (the motion signal acquired at λ_2) is used to estimate the artifacts via an adaptive filter. The artifact-compensated signal is defined as $S_C = S_{PPG} + A - Y$, and the quantity $A - Y$ is minimized via the adaptive filter. We note that Y is a function of S_M (in the simplest case Y and S_M are proportional: $Y = \gamma S_M$ with γ an updated constant that minimizes S_C). Prior to the echo cancellation, the signals were band-pass filtered from 0.75 Hz to 3.5 Hz. In the current prototype, the adaptive filter is a multiplicative coefficient, and the algorithm for updating this coefficient is a Least Mean Square (LMS) solution to minimize the error. In order to determine the heart rate frequency, a Fast Fourier Transform of the signal is calculated.

#121098 - $15.00 USD Received 7 Dec 2009; revised 4 Feb 2010; accepted 17 Feb 2010; published 24 Feb 2010

4. Results

In the lab experiments, the sensors and the light sources were mounted 30 cm away from the skin under investigation. To facilitate optical filtering, the experiment was performed in a dark room. The region of interest consisted of the hand palm, see Fig. 4.

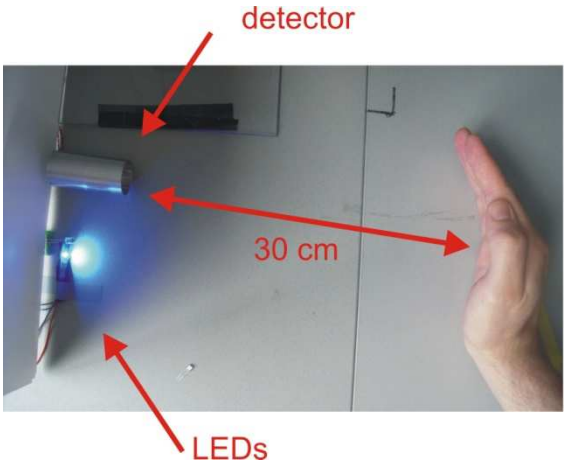

Fig. 4. Measurements set-up. The region of interest is the palm of the hand. The distance bewteen the skin and the detector is 30 cm. Blue and infrared LEDs

Each sensor collected a signal that was sampled at 200 Hz frequency. After the DC removal and the amplification of the AC component, the PPG signal was sent to a PC via USB port. The motion reduction algorithm was performed in real time using the commercial software Matlab (MathWorks^{TM}). We acquired the PPG signals looking at the palm of the hand. The allowed movements of the hands were tilt and translation. The amount of motion was estimated to be between ± 5 degrees around the normal to the detector. This would result in a maximum excursion of the spatial distribution of the backscattered light by 3 cm.

In Fig. 5, we show typical results obtained with our device. The first image shows the two signals from the two photodiodes, Channel 1 (blue) and Channel 2 (IR), in the time domain. The temporal window is 20 seconds long. The graphs in black and in red are the raw signals corresponding to λ_1 = 450 nm λ_2 = 970 nm, respectively. The second image, (b), shows the FFT of the signals in black and red, respectively.

#121098 - $15.00 USD Received 7 Dec 2009; revised 4 Feb 2010; accepted 17 Feb 2010; published 24 Feb 2010

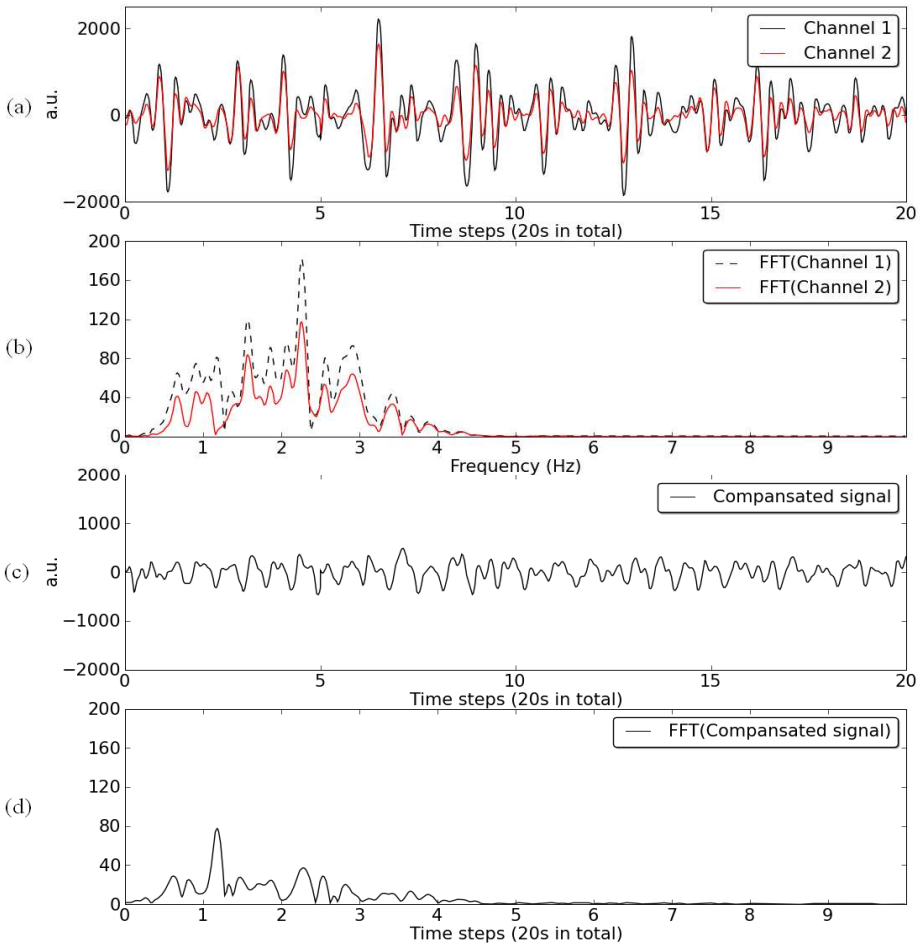

Fig. 5. Results of the motion artifact redution. (a) raw signals from the two photodiodes. (b) frequency spectra of the two raw signals, no clear heart rate component is discernible. (c) compensated signal S_C: a clear "PPG-like" signals is displayed. (d) FFT of the compensated signal, with a clearly visible heart rate component.

We note that from the raw signals it is not possible to discern the heart rate, as the typical photoplethysmographic shape is completely washed out by motion artifacts. In the frequency domain, both FFT spectra (of the raw signals) are broad and display several peaks. The (c) image represents the compensated signal (S_C) we obtain when we apply the signal processing algorithm outlined in paragraph 3.3. We stress that this signal has resemblance of a typical photoplethysmographic signal. The corresponding FFT is displayed in (d). We note that the frequency spectrum of S_C displays a high peak at 1.2 Hz. The higher frequency peaks have been minimized. We note that the motion component with highest frequency (2.2 Hz) has been suppressed by a factor 4.

In order to test the exactness of our artifact reduction, we compared the FFT of the artifacts compensated signal with the FFT of a signal taken when no motion was induced (the hand was kept still). This additional signal was acquired at the same experimental conditions 20 seconds later. This corresponds to the images in Fig. 6, where a clear heart beat frequency at 1.2 Hz and higher harmonics of the heart beat can be discerned as well.

#121098 - $15.00 USD Received 7 Dec 2009; revised 4 Feb 2010; accepted 17 Feb 2010; published 24 Feb 2010

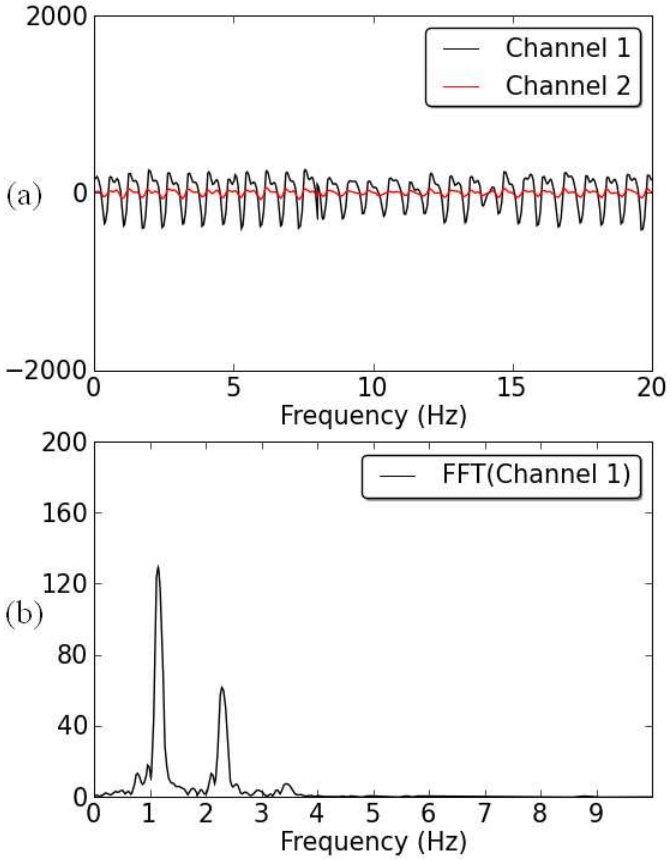

Fig. 6. Photoplethysmographyc signal from the subject without motion. (a) raw signals from the two photodiodes. We can note that the blood volume pulses are more enhanced in one channel. (b) frequency spectrum of the signal in Channel 1. The heasured heart rate is 1.2 Hz.

We can infer the compensated signal display a correct value of heart rate. Moreover, we compared the results of our device with a commercially available oximeter which displayed a value of 86 bpm.

In Table 1, we report the maximum peak frequencies of the FFT of three cases when the motion of the hands had different oscillation frequencies. The Fig. 5 refers to the central column of Table 1. In Table 1, we have considered the frequency components of the FFT with highest contribution.

Table 1. Heart rate measurements with remote photoplethysmograph

Signal	FFT peak (Hz)	FFT peak (Hz)	FFT peak (Hz)
S_{PPG+M}	2.8	2.2	2.1
S_M	2.2	2.2	2.1
S_C	1.2 ± 0.1	1.2 ± 0.1	1.2 ± 0.1

S_{PPG+M} is the signal that contains the PPG and the motion artifacts, S_M contains information about the motion and S_C is the motion artifacts free signal (compensated signal).

The third row of Table 1 shows the maximum peak frequencies of the compensated signals. These values matched the heart rate frequencies measured in absence of motion. We point out that in all three cases, we have considered as error measurement the value of the full width half maximum of the FFT signals. This leads to values of heart beat per minute of 72 ±

#121098 - $15.00 USD Received 7 Dec 2009; revised 4 Feb 2010; accepted 17 Feb 2010; published 24 Feb 2010

6 bpm. The discrepancy between the heart beat valued displayed by the contact oximeter and that obtained with our device is within three times the error we estimate. We anticipate that an opportune signal processing would decrease this discrepancy.

5. Conclusions

We have demonstrated a remote photoplethysmograph that measures heart rate with motion artifact compensation in real time. The device uses two acquisition channels in which the blood pulse volume and the motion induced changes of light intensity are encoded, respectively. The redundancy in the acquired signal has been used for implementation of an adaptive echo cancelation algorithm. The FFT amplitude of the corrected signal showed an improvement of more than 1 order of magnitude with respect to the uncorrected signal. The authors expect that such dual-wavelength technique will be used in all cases of remote photoplethysmography.

Acknowledgments

The authors would like to thank Jeroen Veen, Aad Sempel, and Mark Johnson for the useful discussions and insights.

#121098 - $15.00 USD Received 7 Dec 2009; revised 4 Feb 2010; accepted 17 Feb 2010; published 24 Feb 2010